Conference Paper, Published Version

Rigden, Tom; di Leo, Maria; Grey, Stephen

Big Coastal Physical Models – Controlling Variable Wave Boundaries

Coastal Structures 2019 - Nils Goseberg, Torsten Schlurmann (eds) - © 2019 Bundesanstalt für Wasserbau
ISBN 978-3-939230-64-9 (Online) - DOI: 10.18451/978-3-939230-64-9_118

Big Coastal Physical Models – Controlling Variable Wave Boundaries

T. Rigden, M. di Leo & S. Grey
HR Wallingford, Wallingford, UK

Abstract: In coastal physical modelling, when bathymetries are complex and sea-states vary locally, it becomes necessary to combine all natural features in a single 3D physical model. This leads to physical models requiring long wave generation boundaries over which wave heights and directions could vary significantly. HR Wallingford has developed a novel wave generation method by which the wave height and direction along the paddle can be varied to match target wave parameters along the generation boundary. A recent large physical modelling study of a new port development in Chile, had a wave generation boundary of 5.2 km. The local bathymetry in the model needed to include a deep submarine canyon, which extended several km offshore and reached depths of over 150 m, which lead up to the breakwater of the new port. Due to the canyon, the wave heights along the wave generation boundary varied by 30-40 %. As part of the study, an investigation was carried out to determine the optimal calibration method; whether using variable wave heights and / or variable directions along the paddle front best matched the predicted design conditions at the structure toe. An ARTEMIS numerical model was used as part of the validation and calibration process.

Keywords: Physical modelling, Wave generation, Coastal Structures, ARTEMIS, Breakwater

1 Introduction

The scopes for coastal structure physical models are ever increasing to cover larger and wider areas. Value based engineering is being used to optimize all aspects of the design process, requiring extensive physical model testing to be carried out. This has led more areas of the structures to be sensitive to the expected wave climates predicted over their lifetime. As a result, physical models are being used to verify the design of a greater area of the structures. When the bathymetry and nearshore processes are complex, and sea-states vary locally, it is necessary to combine all the features in a single model.

HR Wallingford recently undertook a large, small-scale physical model study for San Antonio Port Expansion, Chile. This unique site features a large canyon that runs from several km offshore, into the port entrance, reaching a depth of 150 m. The project featured a 3.9 km breakwater with a 2.5 km shore-parallel trunk along which the wave heights varied by over 30-40%. The design of the breakwater reflected this variation with different sized armour designed along different sections of the trunk.

The large sub-marine canyon that led up to the entrance of the new port was an important feature of the local wave climate. It greatly affects the transformation of the waves as they approach the site of the proposed breakwater. The canyon caused the local wave climates along the structure to vary by refracting the waves travelling over it and causing focusing along the breakwater. Along with locally increasing wave heights, the canyon also dispersed the waves in other areas, leading to lower wave heights.

These variations in wave height allowed the designers to optimise the main armour sizes along the breakwater, increasing or decreasing armour size depending on the local wave parameters for a

particular location. The steep sides of the canyon also affected the wave propagation by changing the breaker type of the waves interacting with the breakwater. In particular they caused plunging wave breakers which adversely affect armour stability; another key response included in the model. This effect is similar to that observed and investigated by Shubhra et al. (2008).

The extent of the canyon's influence along the entire trunk of the breakwater needed to be tested as a whole and so it was required that the entire length of the breakwater be included in the model. This required a very large coastal physical model to be carried out at a small scale. Given the size of the structure to be included in the model, the length of approach bathymetry would be close to the recommended limit.

The HDRALAB III guidelines on the physical modelling of breakwaters (HYDRALAB, 2007) provide guidance on the minimum extent of the area to be modelled. The length of the approach bathymetry, between the wave paddle and the test model, is important in ensuring that nearshore processes are properly reproduced. A minimum length of three times the local wave length is recommended.

Since the boundaries of a physical model are limited both horizontally and vertically, it was not possible to include the complete canyon in the model to allow the nearshore processes to be reproduced naturally. The transformations and wave processes happening further offshore therefore had to be simulated at the wave generation boundary. Varying the wave height and direction of the waves at the paddle were seen as potential methods to reduce uncertainty of the short approach bathymetry by adding extra control of the wave generation boundary. A validation of these model controls was carried out using an ARTEMIS numerical model.

In order to simulate the variation in the sea-state within the physical model boundary, the wave parameters for height and direction along the generation boundary – the wave paddles – needed to be varied. HR Wallingford developed a novel wave generation method, and updated its paddle control software, HR Merlin, by which the wave height and direction could be varied to match the target wave parameters along the boundary.

2 Methodology

2.1 Physical model layout

The model was carried out in HR Wallingford's Froude Modelling Hall in wave basins A/B/C. These basins have a combined modelling area of 2,625 m2 and can operate with water depths of 0.8 m. The model was carried out at a scale of 1:100 and covered a prototype area of approximately 18.0 km^2 and approximately 6.5 km of the local coastline and bathymetry. An overview of the model is shown in Fig. 1. The total length of wave generation paddles used in the model was 52 m, equivalent to 5.2 km in prototype.

The submarine canyon was recreated to a depth of -70.0 mNRS. The existing port and surrounding cliffs and headlands were also built and included in the model to ensure the correct boundary conditions were achieved. Waves were generated from three principle offshore directions: WSW, West and WNW. The average inshore direction for each of these directions were: 274ºN, 289ºN and 302ºN, respectively. Wave guides were placed at the edge of the paddles to control diffraction along the edge boundaries.

2.2 ARTEMIS numerical model

An ARTEMIS numerical model was used as part of the validation and calibration of the generated waves. ARTEMIS is a linear finite element wave transformation model, which is used to calculate wave heights in an area of interest corresponding to a given incident wave condition. ARTEMIS was developed by the Laboratoire National d'Hydraulique (LNH) of the Research and Development Division of Electricité de France (EDF-DER) as part of the TELEMAC-MASCARET suite of models (www.opentelemac.com). ARTEMIS is a phase-resolving model based on the mild slope equation (Chamberlain and Porter 1995).

ARTEMIS takes into account the frequency dependence and directional spreading of the wave energy and gives a good representation of the nearshore wave transformation properties which are

recreated in coastal physical models. The different variable sea-state parameters that were defined along the wave generation boundary: variable wave height and direction and spreading were simulated at the numerical model domain boundary in ARTEMIS and compared to the results measured in the physical model.

The ARTEMIS numerical model was set up to replicate the physical model in terms of area covered and input boundary. The same bathymetry that was used to design the physical model was used in the ARTEMIS model. The boundary conditions to the ARTEMIS model were the same as those specified for the physical model. The boundary of the ARTEMIS model can be seen below in Fig. 7.

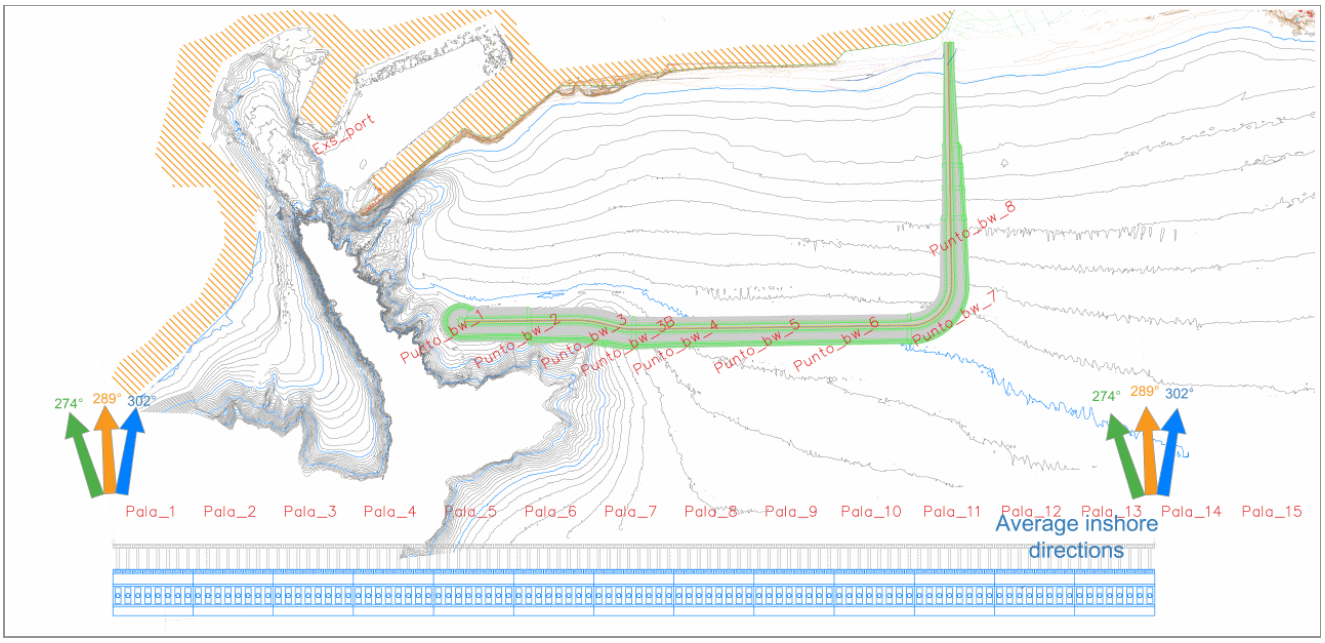

Fig. 1. Physical model layout and location of proposed breakwater and canyon.

2.3 Sea-states

The initial stage of determining the sea-states at the wave generation boundary was to establish the required wave climate at the toe of the breakwater. Using a SWAN numerical model, offshore storm events that would lead to these inshore sea-states were propagated inshore. They were propagated from a mirror point 10 km offshore to the wave generation boundary control points. The SWAN numerical modelling results were provided as part of the physical model data package to be used to calibrate the model.

The sea-states were defined at 13 locations along the wave generation boundary. These locations are shown in Fig. 1 as Pala_1 to Pala_13. At each of these points, the wave height (H_s), period, (T_p), direction (ºN) and spread (σ) were defined. An example of how the sea-states varied along the wave generation boundary and breakwater toe is shown in Fig. 2. This figure shows an example of a sea-state coming from 274°N at the paddle. The highest waves were from around Pala_8 in the middle of the wave generation boundary. These waves transformed inshore to give the largest waves at the toe of the breakwater at bw_4; close to where the bathymetry at the toe of the breakwater rises steeply and transitions from the canyon to a more gentle sloped seabed.

The wave period varied very little across the boundary and had the same average as that found for the corresponding offshore condition. A fixed wave period was therefore used at the generation boundary.

2.4 Variable wave maker

Typically, in a coastal structure physical model, a wave generator will be programmed to generate fixed, non-varying sea-states along its length. Variables such as wave height, period, direction and spreading function will be the same, all along the paddle. The HR Merlin wave generation software

which drives the wave paddles, was updated to allow the wave height and wave front direction to be varied along the length of the wave generator.

The paddle had 104 discreet elements, each 0.5 m wide. The wave paddles were equipped with active wave-absorbing systems to reduce the effect of waves reflected from the test sections, and could generate non-repeating random sea-states of the required spectral JONSWAP form. The wave maker position was fixed along the rear edge of the model boundary, and the variable incoming direction was achieved using the built in paddle steering function.

To control the wave height along the generation boundary, the input gain for each element was adjusted to give the required wave amplitude. The gains were interpolated linearly for the elements between the 13 control points. To generate the curved wave fronts, the delay frequency for each element was calculated based on the elements position along the boundary.

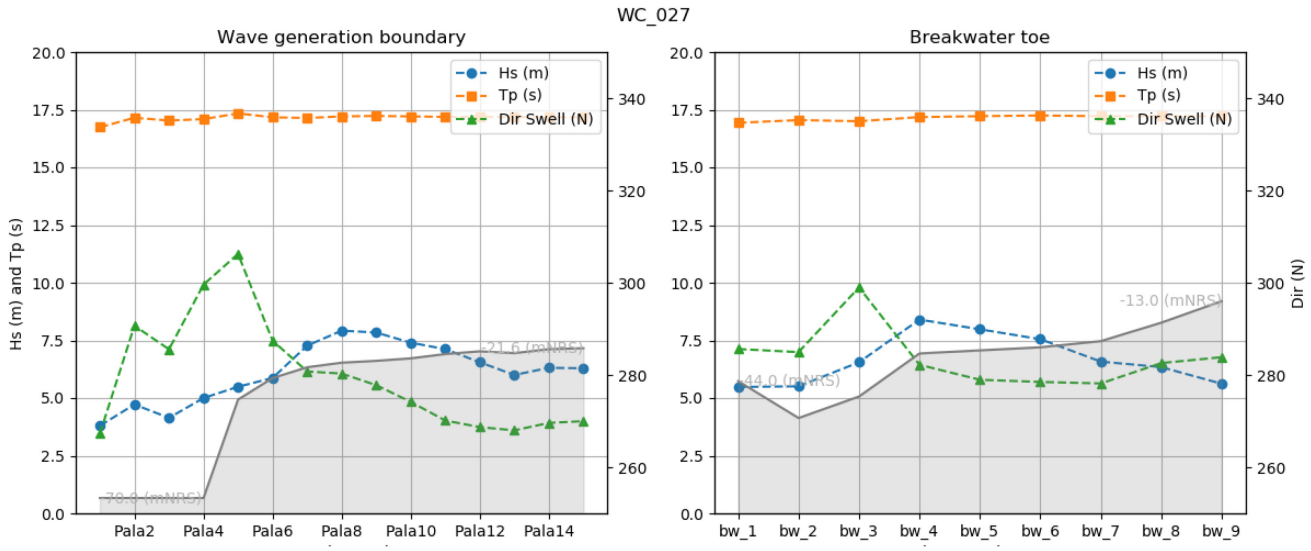

Fig. 2. Sea-state variation along wave generation boundary and breakwater toe.

2.5 *Wave height calibration*

The wave heights at the 13 control points were calibrated using a method similar to that used in a traditional model where a target wave height is matched at a single inshore location. Under these circumstances, it is assumed that the wave transformation from the paddle over the nearshore bathymetry will correctly reproduce the inshore waves. A calibration test was run for 1000 waves, the results were calculated and compared to the target, and the input gain was adjusted until the wave height matched the target for each sea-state calibrated.

An example sea-state calibration output is shown in Fig. 3 which shows the measured wave height against the target wave heights and the gain adjustment factors and interpolated gain values. In this example, the measured values are low around the middle of the generation boundary and so the gains were increased to compensate. The process was repeated until the measured wave heights at all the control points were within ±5.0% of the target.

The wave calibrations were carried out over the test bathymetry before the proposed structures were built. This was to minimise the amount of reflected wave energy in the basin. The wave heights at the control points were measured using single point wave gauges which measure the total wave height including both incident and reflected wave energy. Since it is almost impossible to eliminate all reflected wave energy in a basin, reflection arrays were placed at several locations along the paddle to measure the amount of reflection produced by the model boundaries. An average reflection coefficient of 15% was measured and was applied to the total wave heights measured.

2.6 *Wave direction calibration*

Calibrating the wave direction was more complicated due to the equipment required to determine the direction that waves are travelling. A 10 gauge directional array was used; it was moved to a number of different locations and the tests were repeated. The directions were therefore measured at fewer locations than the wave heights. The directional wave analysis also requires the array to be placed

above an area of flat bathymetry, further reducing the possible locations that the gauge could be placed in the model. Directional measurements were taken along the wave boundary at the wave gauge locations: Pala_7, Pala_9 and Pala_11 as shown in Fig. 1. An image showing the curved wave fronts is shown in Fig. 4, the wave fronts are highlighted in red.

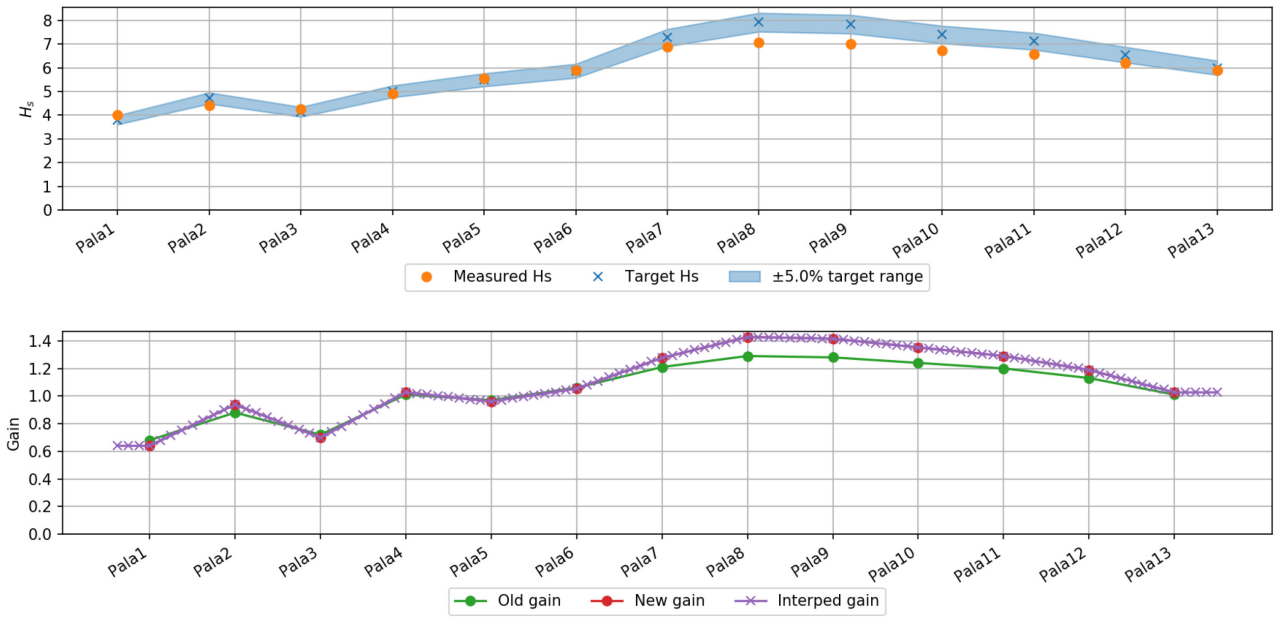

Fig. 3. Sea-state calibration output.

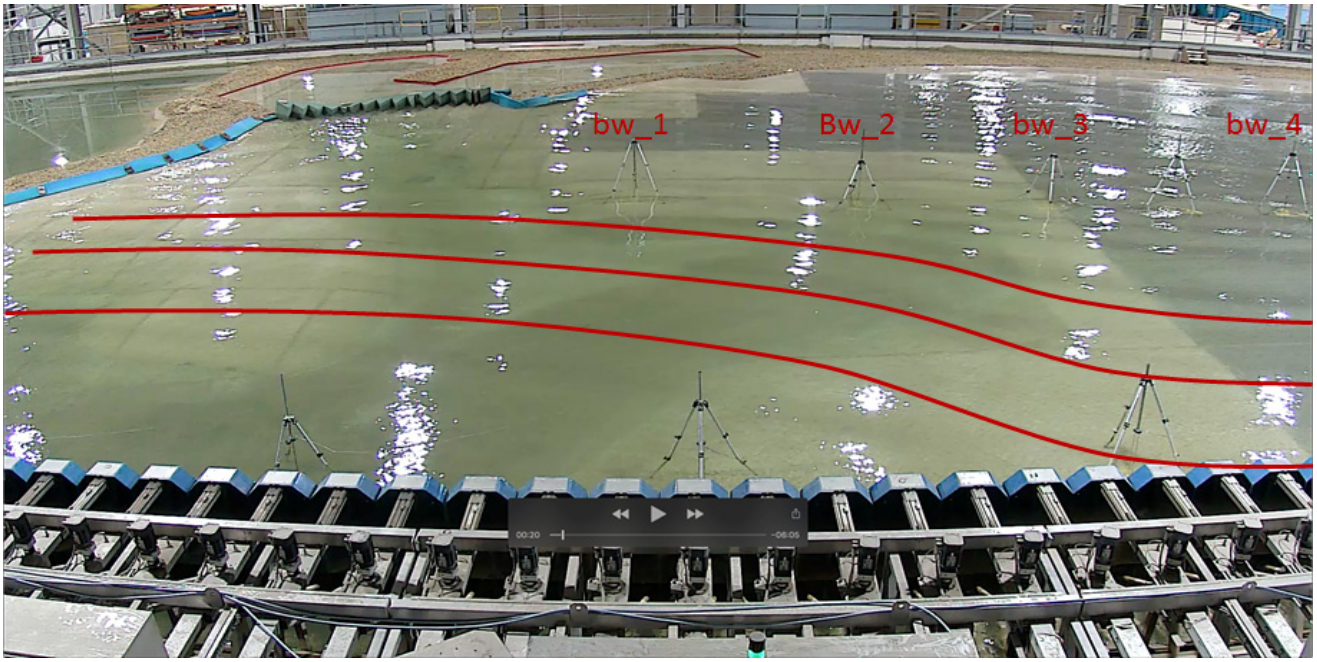

Fig. 4. Curved wave fronts.

3 Results

3.1 Variable wave height calibration

Calibrating the variation in height along the paddle boundary was a simple procedure. The 13 control gains were predicted to give the required variation along the wave generation front. These gains were then interpolated to get the gain for each paddle element. After the first test was run, measured wave heights at the 13 control points were compared to the target wave heights and the control gains were

updated. It was possible to get all 13 control points to match the target within ±5.0 %. Examples of the calibrated wave heights along the generation boundary against the targets is shown in Fig. 5.

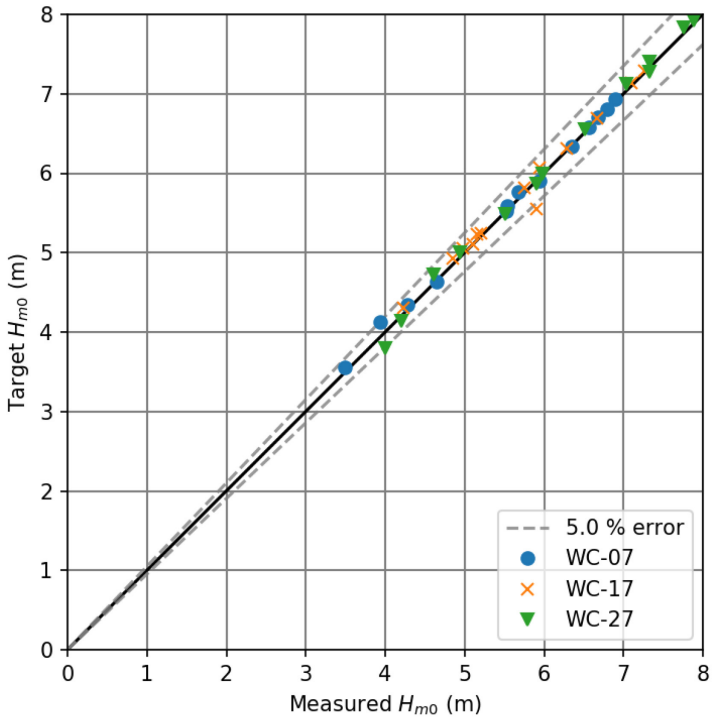

Fig. 5. Sea-state calibration results with variable wave direction (left) and constant wave direction (right).

3.2 Variable direction validation

The measured directions against the target directions are given in Tab. 1. The measurements showed that the paddle was generating a curved wave front as the direction was different directly in front of the wave generation boundary. Comparison with the input direction at each location was generally good with the directions correlating positively. The bathymetry was generally flat in the areas leading to the measurement location but some refraction of the waves could have caused additional curving of the wave front.

Tab. 1. Measured directions and input target direction

Example	WNW		West		WSW	
	Measured (ºN)	Input (ºN)	Measured (ºN)	Input (ºN)	Measured (ºN)	Input (ºN)
Pala_7	312	308	294	294	280	280
Pala_9	304	302	292	290	276	276
Pala_11	300	300	292	290	268	270

3.3 Model sea-state calibration and validation

Three control sea-states were selected to validate the process of varying the sea-states along the wave generation boundary. These conditions were WC-07, WC-17 and WC-27 from West, WNW and WSW sectors, respectively. These sea-states, one from each offshore sector, were representative of a typical design condition for the structure. Tests were run in the physical model in which the wave heights at the 13 control locations along the wave boundary were matched, and then the wave heights at the toe of the breakwater were compared to the numerically predicted wave heights from the SWAN numerical model. This was to validate the variable boundaries effect on the nearshore wave climate.

For the initial set of validation tests, it was assumed that to best represent the predicted sea-states, both the variable wave height and directions should be replicated at the wave boundary control points. The results of calibrating with a variable direction and wave height are shown in Fig. 6. The wave heights were matched to within ±5.0 % of the target for the wave boundary control points. The

measured wave heights at the toe of the structure showed a significant increase between bw_3 and bw_4. This was due to waves focusing as they pass over the canyon, but also the direction in which the waves were steered. Fig. 4 shows the wave fronts generated for WC-17 and the direction the waves is travelling is shown to be towards the wave gauges bw_3 and bw_4. There are also reductions in wave heights around bw_1 and bw_2 which could lead to under-testing the breakwater design.

At the point of focusing, these results differed significantly from the wave heights that had previously been predicted to occur at the toe of the breakwater and used in the design. This would therefore have most likely led to an unrealistic failure of the design structure in this area, potentially due to a modelling effect.

To try and understand better if this focusing was a realistic effect or model effect, the ARTEMIS model was run using the same boundary input conditions with a varying wave height and direction at the generation boundary. The ARTEMIS model showed a similar spike in wave height. The ARTEMIS and physical model results tracked well and followed a very similar pattern. They showed a good relationship between results from the two models. The output of the ARTEMIS model for this set-up is shown in Fig. 7 and the area of wave focusing can clearly be seen.

The calibration process was repeated for these three conditions using a constant wave direction at the paddle equivalent to the average inshore direction. This approach relied on the bathymetry within the model to steer the waves as they approached the toe of the structure. With this set-up, the physical model and ARTEMIS had a good relationship and generally followed the same trend. They were also a better match for the predicted design conditions at the breakwater toe. An area of wave focusing generating an increase in wave height was still observed between Pala_3 and Pala_4 but was less significant.

Since the ARTEMIS model had been showing good correlation with the physical model, this hypothetical scenario was run numerically. The ARTEMIS model was run using an average of the predicted spreading factor across the generation boundary; these values ranged from Cos^7 to Cos^8. Under this scenario, the ARTEMIS model results again differed from those predicted by SWAN at the toe of the breakwater.

The ARTEMIS model was run again using a much broader spreading function equivalent to Cos^2 to Cos^4. With this set-up, the results correlated well with the SWAN model. The results for the broadly spread short-crested waves are shown in Fig. 8.

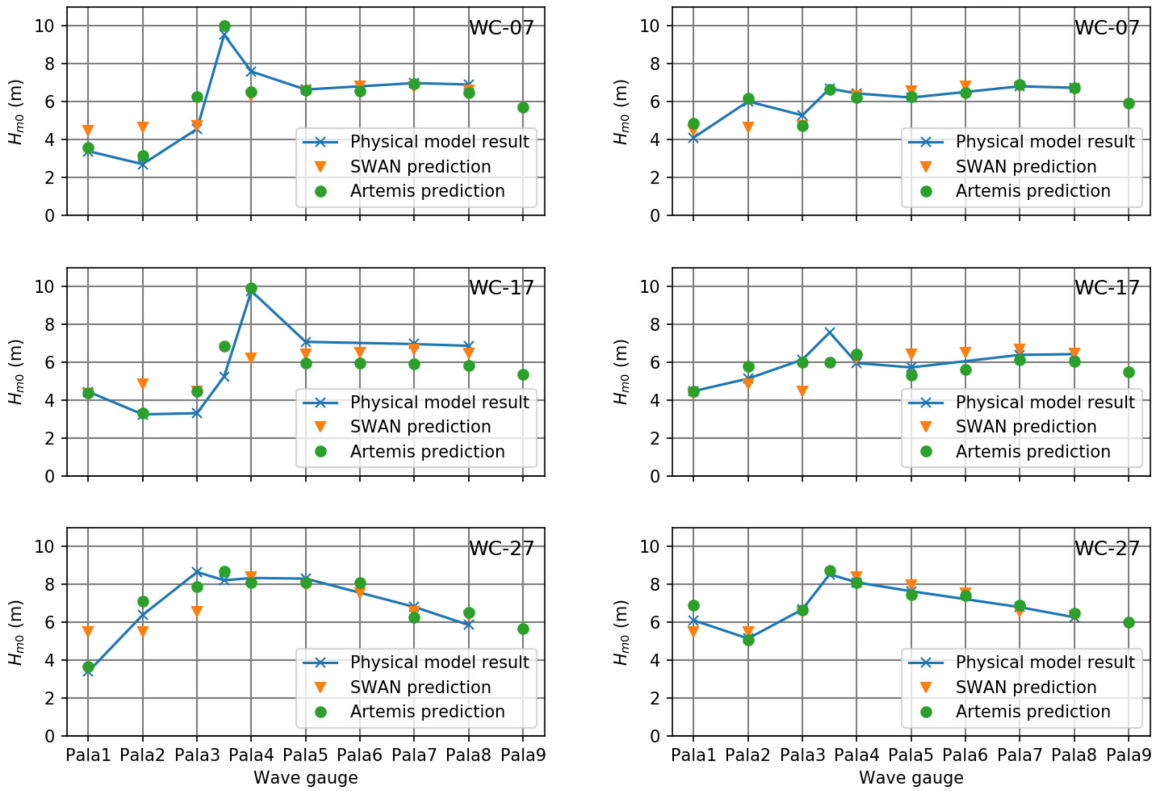

Fig. 6. Sea-state calibration results with variable wave direction (left) and constant wave direction (right).

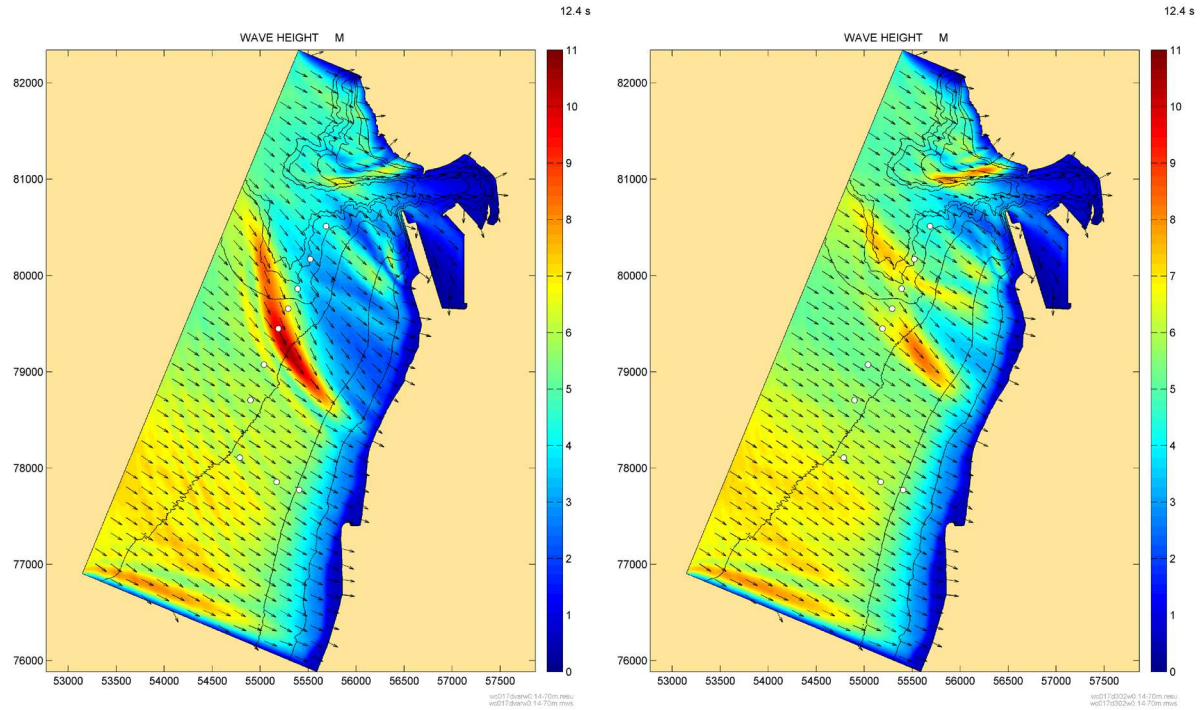

Fig. 7. ARTEMIS model output with variable wave height and direction at generation boundary (left) and fixed wave direction (right) (WC-17).

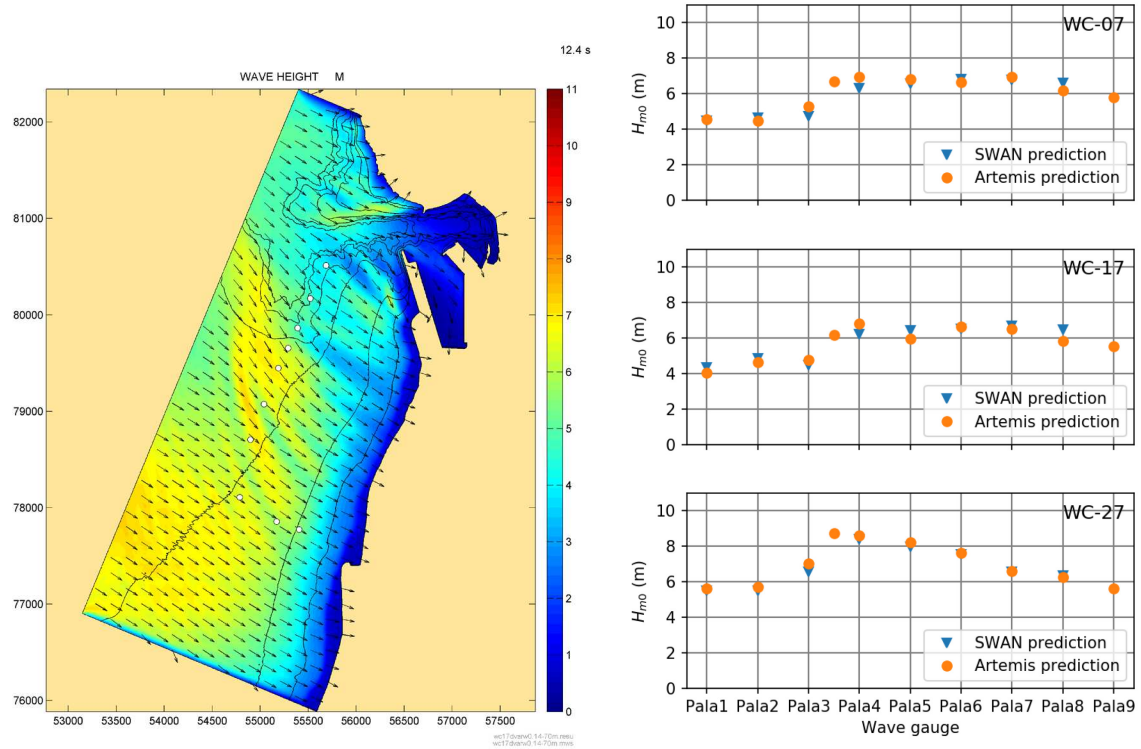

Fig. 8. ARTEMIS model output with variable wave height and direction at generation boundary using short-crested waves (left) (WC-17) and comparison between ARTEMIS and SWAN model results (right).

4 Conclusions

The wave generation system HR Wallingford uses, HR Merlin, was updated to allow variable wave heights and curved wave fronts to be generated at the paddle boundary. This was implemented because of the technical requirements of a large coastal structure physical models. A constant wave generation boundary could not be implemented at a suitable distance away from the test structures to allow the nearshore processes to naturally transform the waves over the approach bathymetry. The

variable wave generation was therefore used to help better simulate the expected inshore wave climate.

Calibration of the variable wave heights was a simple process which was carried out using the principles of the standard procedure whereby a test is run and the input gain is adjusted until the measured wave heights match the target wave height.

The validation of the wave direction was not carried out as comprehensively due to technical requirements whereby a flat bathymetry is required to measure the wave direction and a limitation on available equipment. The checks that were carried out showed that the paddle steering function was able to create a curved wave front that followed the input condition. The results showed that further investigation is needed to fine tune steering according to the target directions to be matched.

The effects of varying the wave generation boundary in a physical model where also validated against an ARTEMIS model. When varying the wave height and or direction at the boundary, the physical model and ARTEMIS had a good correlation. The wave heights measured and predicted at the toe of the breakwater followed a similar trend for the different scenarios run.

For the case study used in this paper, it was not possible to precisely match the predicted conditions at the toe of the breakwater when applying variable wave heights or curved wave fronts at the paddle. This was due to the short-crested spreading function of the waves present at the site which could not be simulated in the physical model; however, a better match to the expected conditions was achieved when only varying the wave height with a constant direction at the paddle for the wave front.

Using a variable wave generation boundary in physical modelling of coastal structures could allow better control of the sea-states generated across the model. This would be particularly useful for very large models with long wave generation boundaries or when approach slope lengths are limited (due to long wave periods or complex local bathymetry). Further investigation should be carried out into the influence on the nearshore processes when forcing predicted wave transformation at the wave generation boundary in a coastal physical model.

References

Shubhra K. Misra, Andrew M. Driscoll, James T. Kirby, Andrew Cornett, Pedro Lomonaco, Otavio Sayao and Majid Yavary. Surface Gravity Wave Interactions with deep-draft Navigation Channels – Physical and Numerical Modeling Case Studies. 31st Int. Conf. on Coastal Engineering (ICCE 2008). Hamburg, Germany.

HYDRALAB, 2007. Guidelines for physical model testing of breakwaters: rubble mound breakwaters. HYDRALAB III Deliverable NA3.1: Version 1.3.

Chamberlain, P.G. and Porter, D., 1995. The modified mild-slope equation. Journal of Fluid Mechanics, 291, pp.393-407.